Low-Temperature Synthesis of TiC, Mo_2C, and W_2C from Modulated Elemental Reactants

Christopher Johnson, Heike Sellinschegg, and David C. Johnson*

Department of Chemistry and Materials Science Institute, University of Oregon, Eugene, Oregon 97403

Received July 5, 2000. Revised Manuscript Received June 6, 2001

The evolution of modulated elemental reactants containing alternating layers of carbon and Ti, W, or Mo was studied using differential scanning calorimetry and X-ray diffraction. TiC crystallized at 350 °C from a modulated reactant with a composition near 1:1 with respect to Ti and C. Mo_2C and W_2C nucleated at 500 and 600 °C, respectively, from modulated reactants with compositions close to their stoichiometry. No exotherms were observed in samples that had compositions that were not close to the stoichiometries of TiC, Mo_2C, or W_2C.

Introduction

The binary transition metal carbides are technologically important materials with a wide variety of applications. The primary use of carbides is as cutting tools and abrasives which take advantage of their immense hardness and chemical stability at high temperatures in ambient atmospheres,[1] but carbides have found applications in many other areas as well. For example, carbide coatings are also used to protect surfaces from erosion and tribological wear as they have good adhesion to substrates and low coefficients of friction as well as high hardness.[1] Tungsten carbide is attractive as a thin film diffusion barrier in the microelectronics industry because of its chemical and thermal stability combined with low electrical resistivity.[2−4] Carbides are used as high-temperature catalysts, with tungsten carbide exhibiting some of the properties of platinum in hydrocarbon conversion reactions as well as having electrocatalytic activity for hydrogen oxidation and oxygen reduction. [5,6] Other properties of carbides that have attracted interest include superconductivity of the molybdenum carbides as well as the magnetic properties of $Y_2Fe_{17-x}M_x$ type carbides[7] that have been proposed as candidate materials for high-performance permanent magnets.

As a consequence of their useful properties, numerous synthetic approaches have been explored to prepare binary carbides. The initial synthesis of most of the refractory carbides in the late 1800's was by high-temperature (1500−2000 °C) reduction of the oxides with carbon.[1] With many of the early transition metal systems this synthesis approach results in the formation of oxycarbides, and the removal of the last traces of oxygen from the carbides is very difficult. In the 1940s and 1950s, it was found that many of the carbides could be prepared by high-temperature reaction between hydrocarbons and either the oxides or metals. Again, removal of oxygen from the resulting products was difficult. To eliminate the incorporation of oxygen, later work focused on the direct reaction of the elements by arc melting or by heating the powdered elements to temperatures exceeding 1000 °C. The high reaction temperatures in either of these approaches were necessary to break the strong carbon−carbon bonds in the carbon containing reactant as well as the metal−metal or metal−oxygen bond in the metal containing reactant. The high reaction temperatures also speed up product formation by increasing the rate of carbon diffusion through the intervening product carbide formed on the surface of the reacting metal.

In the past 20 years, several new approaches have been developed for the synthesis of bulk carbides. Most prominent among these is the use of self-propagating, high-temperature reactions, developed in the Soviet Union during the late 1960s and 1970s. This method takes advantage of the large heats of formation of the carbides from the elements. The reaction is initiated by locally heating a compact containing intimately mixed elemental powders and then sustains itself in the form of a reaction wave with temperatures on the order of 2000−3000 °C occurring at the reaction front because it is a highly exothermic reaction.[8] More recently, chemical vapor deposition with organometallics as single source precursors has been used to prepare carbide films for protective coatings or diffusion barriers at relatively low temperatures (350−600 °C).[9] Yet another successful moderate temperature (600−1000 °C) approach has been the preparation of carbides with large surface areas by reaction of oxide aerogels with methane.[10] The high reaction temperatures in the self-

(1) Schwarzkof, P.; Kieffer, R. *Refractory Hard Metals: Borides, Carbides, Nitrides and Silicides*; MacMillan Co.: New York, 1953.
(2) Murarka, S. P. *J. Vac. Sci. Technol.* **1980**, *17*, 775−792.
(3) Yan, H. Q.; Zhao, X. A. *J. Vac. Sci. Technol. A* **1988**, *6*, 1646.
(4) Ghaisas, S. *J. Appl. Phys.* **1991**, *70*, 7626.
(5) Ribeiro, F. H.; Betta, R. A. D.; Boudart, M.; Baumgartner, J.; Iglesia, E. *J. Catal.* 1991, *130*, 86.
(6) Nikolov, I.; Papazov, G.; Pavlov, D.; Vitanov, T.; Naidenov, V. *J. Power Sources* 1990, *31*, 69.
(7) Laforest, J.; Burzo, E.; Valeanu, M.; Plugaru, N. *J. Magn. Magn. Mater.* **1995**, *140/144*, 973.
(8) Munir, Z. A. *Ceram. Bull.* **1988**, *67*, 342−348.
(9) Lai, K. K.; Lamb, H. H. *Chem. Mater.* **1995**, *7*, 2284−2292.

10.1021/cm000547c CCC: $20.00
Published on Web 09/19/2001

propagating reactions and the conversion of oxide aerogels again result from the need to increase the diffusion rate of carbon through the intervening product carbide.

Our approach to overcoming slow diffusion rates in the synthesis of solid-state compounds has been the use of modulated elemental multilayers in which the layer thickness of the individual elements is on the order of angstroms.[11] The short diffusion lengths result in complete interdiffusion at low temperatures and amorphous intermediates in metal−silicon, metal−selenium, and metal−metal systems that can be kinetically trapped. In these amorphous reaction intermediates, nucleation is the rate-limiting step in forming crystalline solids and the activation energy for nucleation is a function of the composition of the amorphous intermediate.[12] In systems containing compounds with similar nucleation energies, the overall composition of the amorphous intermediate can be altered to selectively prepare desired compounds directly from the amorphous reaction intermediate.[13] Ternary compounds can be directly nucleated from ternary amorphous intermediates, avoiding the formation of stable binary compounds as reaction intermediates.[14] By controlling diffusion lengths and local composition within the initial modulated elemental reactant, it is also possible to kinetically trap crystalline superlattices with designed superstructure.[15]

High-quality modulated multilayers with periodicities in the range of 10−100 Å containing carbon with tungsten, molybdenum, chromium, titanium, vanadium, and nickel have previously been prepared for use as soft X-ray monochromators and reflectors. [16,17] Since roughness of the interfaces and stability of the modulated structure is critical for this application, several studies have addressed these points. The deposited carbon has been found to be amorphous, and if the metal is thin enough, for example 10 Å in the case of tungsten, it has also been found to be "amorphous". The "amorphous" metal in these systems is thought to be a metal−carbon alloy. Given the large negative heats of mixing found in the carbides, it was predicted that many metal−carbon systems should undergo solid-state amorphization reactions. Annealing tungsten−carbon multilayers, the most studied system, produced a variety of tungsten carbide phases at temperatures from 350 to 750 °C.[18]

The results published in the literature on the metal−carbon multilayers discussed above suggest several promising applications for modulated elemental reactants in carbide synthesis. For example, low-temperature access to carbides using modulated elemental reactants could extend the use of carbides as protective coating and thin film diffusion barriers to temperature sensitive substrates. A survey of the literature suggests that the scarcity of known ternary carbides is a consequence of thermodynamic and chemical stability of the binary carbides. This suggests that modulated elemental reactants might provide a fruitful avenue for exploratory synthesis of ternary carbides, providing a means to avoid the formation of binary carbides as intermediates. Finally, the improvements found in the properties of mixed metal solid solution carbides, for example elevated melting points and enhanced chemical stability, suggest that nanolaminated binary carbides might enhance desired properties even further. Modulated elemental reactants can be used to kinetically trap such nanolaminated products as well as to control the structure of the periodicity because one can design the initial reactant structure.

The first step in exploring these promising research directions is to determine how the binary metal−carbon systems react and whether one can control the reaction mechanism by adjusting the structure of the initial reactant. In this paper we discuss the reaction pathways of three systems (titanium−carbon, molybdenum−carbon, and tungsten−carbon) and explore the effect of the structure of the initial multilayer reactant upon the reaction pathway.

Table 1. Mo/C Samples and Intended Thicknesses

	intended thickness, Å		
sample ID	C	Mo	composn %C:%Mo
MoC 1	4.0	7.1	79.7:20.3
MoC 2	4.0	13	74.2:25.8
MoC 3	4.0	16	70.1:29.9
MoC 4	4.0	18	62.5:37.5
MoC 5	2.3	17	54.1:45.9
MoC 6	2.3	21	48.3:51.7
MoC 7	2.3	25	42.4:57.6
MoC 8	2.3	30	35.8:64.2

Table 2. Ti/C Samples and Intended Thicknesses

	intended thickness, Å		
sample ID	C	Ti	composn %C:%Ti
TiC 1	2.3	4.5	79:21
TiC 2	2.3	7.5	72:28
TiC 3	2.3	10	63:37
TiC 4	2.3	13	52:48
TiC 5	2.3	15	40:60
TiC 6	2.3	19	26:74

Experimental Section

Sample Preparation. The carbon−metal samples for these studies were prepared using a custom built ultrahigh vacuum chamber. The various elements were evaporated at a rate of 0.5 Å/s using electron beam gun sources independently controlled by quartz crystal thickness monitors. To obtain a range of compositions for each binary system, the intended thickness of carbon was held constant while the thicknesses of the various metal layers were varied, as shown in Tables 1−3. Multilayered samples were simultaneously deposited on polymethylmethacralate (PMMA) coated silicon wafers and on uncoated silicon pieces. Total film thicknesses were all larger than 500 Å to obtain sufficient sample mass for thermal analysis. The layers deposited on the PMMA coated wafers were removed from the substrate by dissolving the PMMA in acetone. The sample was collected on a Teflon filter, creating a sample free of the substrate for thermal analysis. The sample deposited straight on silicon was used for low-angle X-ray diffraction studies.

(10) Teixeira da Silva, V. L. S.; Ko, E. I.; Schmal, M.; Oyama, S. T. *Chem. Mater.* **1995**, *7*, 179−184.
(11) Johnson, D. C. *Curr. Opin. Solid State Mater. Sci.* **1998**, *3*, 159−167.
(12) Fukuto, M.; Hornbostel, M. D.; Johnson, D. C. *J. Am. Chem. Soc.* **1994**, *116*, 9136−9140.
(13) Oyelaran, O.; Novet, T.; Johnson, C. D.; Johnson, D. C. *J. Am. Chem. Soc.* **1996**, *118*, 2422−2426.
(14) Schneidmiller, R.; Bentley, A.; Hornbostel, M. D.; Johnson, D. C. *J. Am. Chem. Soc.* **1999**, *121*, 3142−3149.
(15) Noh, M.; Johnson, D. C. *Angew. Chem., Int. Ed. Engl.* **1996**, *35*, 2666−2669.
(16) Falco, C. M.; Fernandez, F. E.; Dhez, P.; Khander, A.; Nevot, L.; Pardo, B.; Corno, J. 1987.
(17) Falco, C. M. In *Growth of metallic and metal-containing superlattices*; Dhez, P., Weisbuch, C., Eds.; Plenum Press: New York, 1988; Vol. 182, pp 3−15.
(18) Lamble, G. M.; Heald, S. M.; Sayers, D. E.; Ziegler, E.; Viccaro, P. J. *J. Appl. Phys.* **1989**, *65*, 4250−4255.

Table 3. W/C Samples and Intended Thicknesses

	intended thickness, Å			intended thickness, Å	
sample ID	C	W	sample ID	C	W
WC 1	1.6	19	WC 9	1.6	1.9
WC 2	1.6	37	WC 10	1.6	20
WC 3	1.6	56	WC 11	1.6	22
WC 4	1.6	9	WC 12	1.6	24
WC 5	1.6	19	WC 13	0.8	11
WC 6	1.6	28	WC 14	1.2	17
WC 7	1.6	17	WC 15	1.2	17
WC 8	1.6	19	WC 16	2.3	33

Composition Analysis. The average composition of the multilayer films was determined by electron microprobe analysis using an energy-dispersive X-ray detector.

X-ray Diffraction. Diffraction data were collected on a Scintag XDS 2000 $\theta-\theta$ diffractometer using Cu Kα radiation. The sample stage of this diffractometer has been modified to allow for rapid and precise alignment for low-angle diffraction studies. The low-angle diffraction data were collected to determine if the samples contained a periodic layered structure, to measure total film thickness, and to obtain an estimate of the roughness of the deposited film. High-angle diffraction data were used to determine whether the as-deposited, substrate free, and annealed samples contained crystalline elements or compounds.

Differential Scanning Calorimetry. Differential scanning calorimetry (DSC) data were collected using a TA Instruments TA 9000 calorimeter fitted with a 910 DSC cell. An initial scan ramped from 50 to 600 °C at a rate of 10 °C/min was performed on all samples. Additional portions of samples were scanned in the calorimeter to temperatures just above or below the observed exotherms and subsequently X-rayed to obtain information on structural changes resulting in heat evolution. DSC data above 550 °C were collected on a Polymer Laboratories STA 1500 DSC at heating rates of 2−25 °C/min up to 1200 °C.

Transmission Electron Microscopy. Crystallinity of the samples was also examined using through foil transmission electron microscopy (TEM) where free-standing sample films were mounted on standard copper grids. The TEM instrument used was a Philips CM12 operated at an accelerating voltage of 100 keV.

Results and Discussion

The initial deposition data for the transition metal−carbon multilayer samples prepared for these studies are summarized in Tables 1−3. The intended layer thickness of all the samples is listed. Low-angle X-ray diffraction data were collected on each sample to determine the actual repeat layer thickness. Unfortunately, diffraction maxima resulting from the interference between X-rays scattered from the front and the back of the deposited sample were only observed in some of the samples. For the samples contained in Tables 1−3 the first-order Bragg diffraction maxima resulting from the compositional modulation in the as-deposited sample were also not observed. The composition of the Ti−C and Mo−C samples was determined using electron microprobe analysis. There was not enough sample available to perform this measurement on the W−C samples. Tables 1−3 summarize the information obtained on the transition metal−carbon multilayers prepared. The percentage of the transition metal composition increases as expected when the thickness of the deposited transition metal is increased. Graphing the composition versus the intended metal thickness permits us to extract information concerning the ratio of carbon to transition metal thickness of the elemental layers. Using a tooling factor (the actual amount of the element deposited on the sample substrate relative to that deposited on the crystal monitor due to the deposition geometry) for the transition metals obtained in previous studies, a tooling factor for carbon could be determined. This was then used to determine the actual carbon layer thickness from the intended layer thickness. The calculated repeat layer thicknesses determined from the low-angle diffraction scans, when observable, are generally in good agreement with the intended repeat layer thicknesses calculated using the tooling factors determined from the composition data.[19]

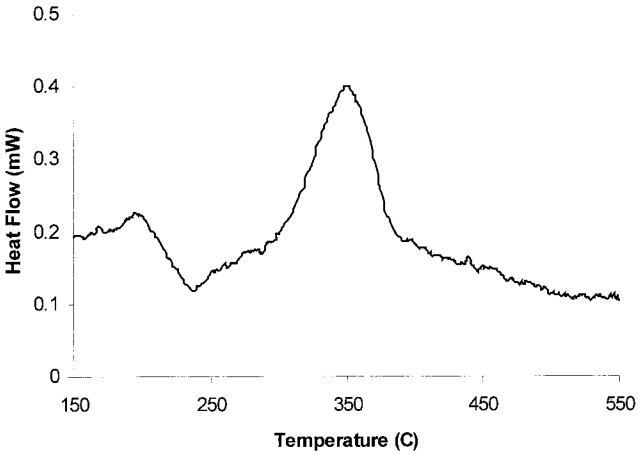

Figure 1. Differential scanning calorimetry data collected on a Ti/C multilayer (sample Ti−C 4 as shown in Table 1). An exotherm is visible at a temperature of 350 °C.

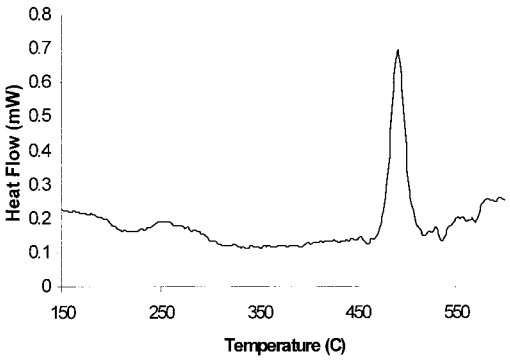

Figure 2. Differential scanning calorimetry data collected on a Mo/C multilayer (sample Mo−C 8 as shown in Table 2). An exotherm is observed at 500 °C.

DSC data were collected on all of the samples to obtain initial information on their evolution as a function of temperature. For the titanium−carbon samples, an exotherm was observed at 350 °C for sample Ti−C 4, as shown in Figure 1, while no exotherms were observed in any of the other samples. In the molybdenum−carbon system, an exotherm was observed in sample Mo−C 8 at 500 °C, as shown in Figure 2, while no exotherms or endotherms were observed in any of the other Mo−C samples. In the tungsten−carbon multilayers, an exotherm was observed in sample WC 5 at 600 °C, as shown in Figure 3, while, again, no exotherm was observed in the other W−C samples.

(19) Hornbostel, M. D.; Hyer, E. J.; Thiel, J. P.; Johnson, D. C. *J. Am. Chem. Soc.* **1997**, *119*, 2665−2668.

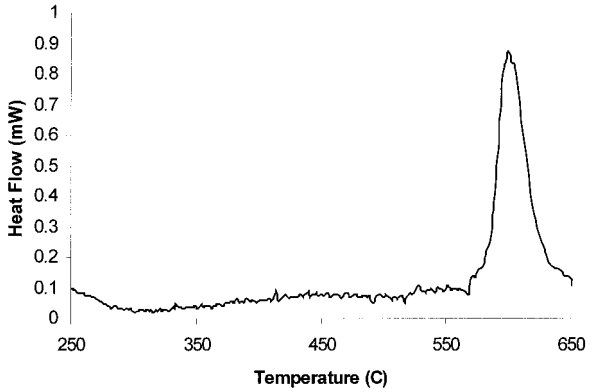

Figure 3. Differential scanning calorimetry data collected on a W/C multilayer (sample W−C 5 as shown in Table 3) with an exotherm observed at 600 °C.

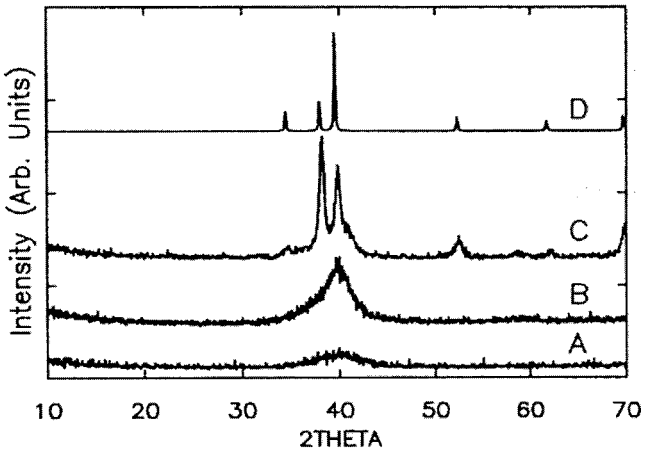

Figure 4. X-ray diffraction data collected as a function of annealing temperature on the Mo/C multilayer used in the DSC experiment shown in Figure 2. The labels indicate temperatures in the DSC experiment: A = as-deposited; B = 450 °C; and C = 600 °C. The curve labeled "D" represents the JCPDS diffraction file simulation for α-Mo_2C.

High-angle X-ray diffraction data were collected both before and after the DSC scans on all of the samples to determine the structural changes that occurred on heating. The as-deposited diffraction scans of all of the samples indicated that they were amorphous on deposition. Diffraction scans of the samples which did not contain an exotherm in the DSC showed that the samples remained amorphous even after heating to 550 °C. For samples having exotherms in their DSC scans, diffraction scans were collected immediately before and after the exotherm temperature. High-angle diffraction data as a function of annealing temperature for samples MoC-8, WC-5, and TiC− 4, which did display exotherms, are shown in Figures 4−6.

The samples containing exotherms from each of these systems all evolved in a very similar manner. Diffraction scans performed on these samples heated to a temperature just below the observed exotherms show only small changes compared to the as-deposited samples, containing broad and weak diffraction maxima characteristic of noncrystalline materials. The diffraction scans collected on these samples after heating to temperatures above the exotherm showed clearly that the samples had crystallized. The diffraction patterns of the crystallized samples Ti−C 4, Mo−C 8, and W−C 5 matched the JCPDS diffraction patterns for TiC, Mo_2C, and W_2C,

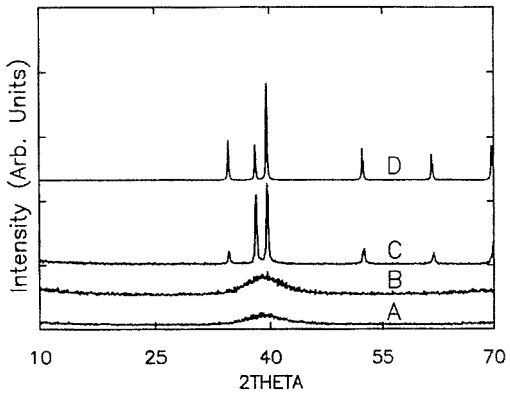

Figure 5. X-ray diffraction data collected as a function of annealing temperature on the Ti/C multilayer used in the DSC experiment shown in Figure 1. The letters indicate the temperature to which the sample was heated in the DSC experiment: A = as deposited; B = 300 °C; and C = 550 °C. The upper curve is a simulation of the JCPDS diffraction file for TiC.

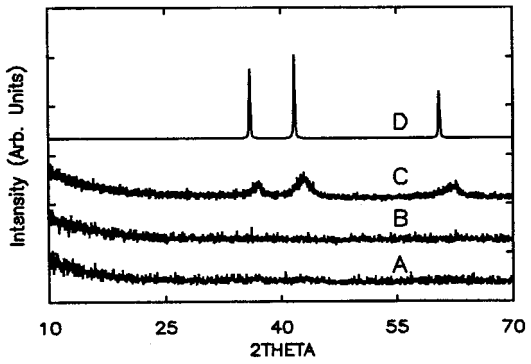

Figure 6. X-ray diffraction data collected as a function of annealing temperature on a W/C multilayer used in the DSC experiment shown in Figure 3. The labels indicate temperatures to which the samples have been heated. A = as deposited; B = 500 °C; and C = 700 °C. The upper curve is the JCPDS diffraction file simulation for W_2C.

respectively. We cannot distinguish between the α or β phases of Mo_2C and W_2C due to the large width of the observed diffraction maxima.

The samples that did not display exotherms after heating to 550 °C were heated to 1200 °C to determine if any other crystalline compounds would form. All of the samples studied eventually crystallized after high-temperature annealing. The remaining Ti−C samples formed TiC, and, for titanium rich samples, some crystalline titanium was also observed. The diffraction scans of the Mo−C samples showed only the formation of Mo_2C and in some cases crystalline molybdenum even though the samples were carbon rich in comparison to Mo_2C. The diffraction data showed no evidence for the formation of MoC in samples heated to 1200 °C. The diffraction scans of the W−C samples also showed only the formation of W_2C and in some cases crystalline tungsten, again, even in samples that were carbon rich in comparison to W_2C.

This lack of selectivity as a function of composition is surprising considering that previous studies on nucleation as a function of sample composition showed that composition controlled phase formation.[20] There are at least two ways to explain this phenomenon. First, the large heat of formation of the TiC, Mo_2C, and W_2C

phases relative to other crystalline phases potentially provides enough driving force for crystallization of these compounds, even at compositions far removed from their ideal stoichiometries, so that the crystallization of other compounds is suppressed. The activation energy for nucleation is smaller for compounds with higher heats of formation. The size of a critical nucleus is also inversely related to the heat of formation. Thus, critical nuclei of these compounds will be smaller and require lower activation energy to form than other compounds in the respective binary phase diagrams. A second possibility is that the binary compounds are interfacially nucleating at the reacting interfaces, implying that the samples have not completely interdiffused before nucleation even occurs. Usually low-angle Bragg diffraction maxima of the multilayers would establish whether samples interdiffuse to a homogeneous amorphous intermediate before crystallization or whether the samples nucleate interfacially before the layers interdiffuse entirely. If a sample interdiffuses to form an amorphous intermediate before nucleation, the low-angle Bragg maxima disappear at temperatures below the observed nucleation temperature marked by the exotherm in a DSC scan. If the sample interfacially nucleates, we observe low-angle Bragg diffraction concurrent with high-angle diffraction maxima resulting from the crystalline compound. In the present case, however, this determination is made more difficult by the lack of the low-angle diffraction maxima that are expected to result from the elemental modulation. This may be a result of interdiffusion of the layers on deposition, from too much interfacial roughness due to the cumulative effect of sequential deposition on a cold substrate, or from a combination of these effects. If interdiffusion is the cause of the missing Bragg peaks, preparing samples with thicker elemental layers should result in observable diffraction maxima. If cumulative roughness is the complication, preparing samples with fewer repeating layers should result in observable Bragg diffraction maxima.

We examined this issue of interfacial nucleation versus homogeneous nucleation most thoroughly in the Mo−C system. We prepared a modulated Mo−C sample with fewer (20) but thicker (30 Å) repeating layers of Mo and C in an attempt to prepare a sample with observable low-angle Bragg diffraction maxima. The combination of both of these changes resulted in the ability to follow the interdiffusion of this sample by the decay of the diffraction peaks. The data obtained on annealing the sample for 30 min at 450 °C are shown in Figure 7. The scan of the as-deposited sample contains the first-order Bragg diffraction maxima at 2.73° 2θ and a set of diffraction maxima resulting from a combination of incomplete destructive interference of the diffraction from the layers due to the small number of deposited layers and the interference of the X-rays scattered from the top of the multilayer and the interface between the sample and the substrate. The position of the Bragg diffraction maxima allows us to determine the layer spacing using Bragg's law—32.3 Å. The lack of higher order Bragg diffraction maxima suggests that the interface region between the layers

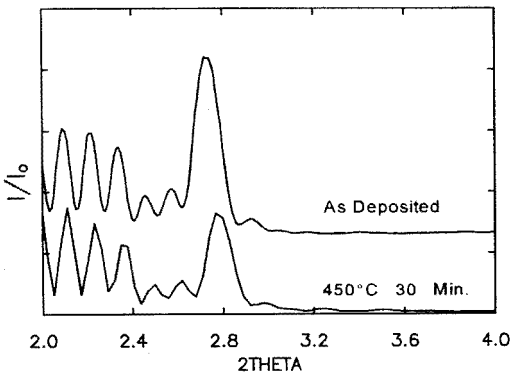

Figure 7. Low-angle diffraction pattern collected on a Mo/C multilayer with a repeat layer spacing of 30 Å. The upper scan was collected on the as-deposited sample, and the lower scan was collected on the sample after it had been annealed for 30 min at 450 °C.

is broad—needing little if any of the second Fourier component with a length scale of 16 Å to describe the electron density profile at the interface. A second explanation of the lack of higher order Bragg diffraction maxima is that the interfacial regions are too rough to give coherent diffraction at a length scale of 16 Å. The roughness of both the sample−air interface as well as the sample−substrate interface can be determined by the decay of the interference maxima resulting from these interfaces as a function of 2θ. Wainfan and Parratt developed a relationship between the angle at which the interference maxima are no longer observable and the roughness of the interfering surfaces as shown in

$$\Delta t = \lambda/[4(\theta_n^2 - \theta_c^2)^{1/2}] \quad (1)$$

where $\lambda = 1.54$ Å, θ_n is the fringe maximum at the nth order and θ_c is the critical angle.[21] The absence of the diffraction maxima at a 2θ angle of 3.2° suggests an average roughness of ∼14 Å.[22] Since the sample was deposited on a polished silicon wafer with a root mean square roughness of ∼3 Å, we attribute the majority of the observed roughness to the surface of the deposited sample.

Several changes are readily apparent in the diffraction pattern of the sample on annealing. First, the position of the diffraction maxima has shifted to a higher diffraction angle. This shift implies that the sample has contracted, with the average Mo−C bilayer distance being decreased to 31.7 Å, a contraction of 0.6 Å. We believe that this decrease is a result of mobile vacancies diffusing out of the sample on annealing. The as-deposited state of an evaporated element is typically 3−5% less dense than the bulk values because the condensing atoms are not given sufficient time to diffuse on the surface to find an ideal location before becoming buried by the subsequent flux of atoms. We believe most of the contraction is a result of this phenomenon. Second, the intensity of the first-order Bragg diffraction maximum has decreased by a factor of 2 during the 30 min anneal at 450 °C. Since the intensity of the first-order diffraction peak is directly proportional to the

(20) Johnson, C. D.; Anderson, K.; Gromko, A. D.; Johnson, D. C. *J. Am. Chem. Soc.* **1998**, *120*, 5226−5232.

(21) Wainfan, N.; Parratt, L. G. *J. Appl. Phys.* **1960**, *31*, 1331−1337.

(22) Zeppenfeld, A. C.; FIddler, S. L.; Ham, W. K.; Klopfenstein, B. J.; Page, C. J. *J. Am. Chem. Soc.* **1994**, *116*, 9158−9165.

electron density difference between the Mo rich region and the C rich region of the bilayers, we conclude that significant interdiffusion of Mo and C occurs as a result of the elimination of vacancies during the annealing process. The width of the diffraction maxima did not change on annealing, suggesting that the diffusion is mainly planar—remaining parallel to the substrate on annealing. This and the lack of high-angle diffraction maxima from a crystalline material suggest that grain growth of any crystalline compound has not occurred during the annealing. Third, we note that the interference maxima can now be observed out to 3.6° 2θ, suggesting that the average roughness of the top of the sample has decreased to ~12 Å. This again suggests that no crystalline compounds have nucleated at the reacting interfaces because grain growth would be expected to increase interfacial roughness. Since we find no evidence for reaction of the sample with the polished silicon wafer, we attribute the change in the observed roughness to smoothing of the deposited layers.

The interdiffusion study gave us important information concerning the evolution of the reacting Mo−C interfaces. From these data we can imply that significant interdiffusion of Mo rich and C rich regions of the samples in Table 2 occur on annealing. Since diffusion time varies with the square of diffusion length, we would expect the composition gradients to be decreased by factors of 10−20 in the samples contained in Table 2 on annealing at 450°C for 30 min. If nuclei larger than the critical size were present in the sample, we would have expected rapid growth of these crystallites. However, this was not observed, suggesting that no nuclei were present. All of these data strongly indicate that the samples contained in Table 2 interdiffuse before nucleating. This is also consistent with the sharp exotherms observed during crystallization that implies a fast growth of the crystalline phase. This suggests that little diffusion is required at the fronts to deliver nutrients to the growing crystals. There was, however, one piece of conflicting data. The intensity of the 200 diffraction peak (assuming α Mo_2C) in the diffraction pattern of the crystalline Mo_2C from both samples Mo−C 7 and Mo−C 8 is more intense than would be expected from a sample with randomly oriented crystallites. The full width at half-maximum (fwhm) of rocking curve scans of the 200 peaks of both samples have a fwhm of only 9° 2θ, confirming the preferred orientation of the crystallites. The only explanation that seems consistent with these data is that some influence of the initial interfacial structure is still present during nucleation. This implies that complete mixing by diffusion has not taken place. The diffraction data obtained on W_2C formed during the low-temperature exotherm in W−C 5 also suggests preferred nucleation of crystallites with orientation of 200 planes parallel with the original layering direction. In previous studies where interfacial nucleation has been observed, the crystallite size of the resulting compounds has been determined by the thickness of the deposited layers.[12] This is not the case in the present study, as the crystallites are at least a factor of 10 larger than the single repeat layer thickness. Thus, if the samples nucleate at the reacting interfaces, the nucleation density is very low during the time required for crystal growth of the first formed nuclei.

We observed two interesting trends that connect both nucleation and growth to the heats of formation of the binary carbides formed. The nucleation temperature scales inversely with the heat of formation of the compounds. TiC, which has the largest heat of formation of the three binary carbides formed, has the lowest nucleation temperature. W_2C, which has the smallest heat of formation, has the highest nucleation temperature, and Mo_2C lies between these extremes. This trend results from the correlation of the heat of formation, critical nucleus size, and activation energy required for crystallization. The second trend observed is that the crystallite size scales inversely with the heat of formation. TiC, which has the highest heat of formation (and the lowest nucleation temperature), forms crystallites of only 100 Å, as estimated from the diffraction peak broadening. The crystallite sizes increase as the heat of formation decreases as we go to Mo_2C and W_2C. This second trend is most likely due to the exponential Arrhenius-like temperature dependence of diffusion rates. The slower growth of crystals at lower temperatures permits more nuclei to form.

Summary

The results presented demonstrate the ability to form carbides at low temperatures using modulated elemental reactants. To form crystalline compounds at low temperatures, the composition of the samples must be near the stoichiometry of the intended compounds. Only the carbide phases with the highest heats of formation were observed to crystallize. The available data leave open the question of whether the samples nucleate interfacially at the reacting interfaces or formed via nucleation from a more homogeneous amorphous intermediate.

Acknowledgment. The support of the National Science Foundation (DMR-9510562 and DMR-9813726) is gratefully acknowledged. The help and assistance of Mr. Michael Shaffer with the elemental analysis using electron microprobe equipment is greatly appreciated.

CM000547C